

DISCOVERY OF FULMINIC ACID, HCNO, IN DARK CLOUDS¹

NÚRIA MARCELINO², JOSÉ CERNICHAO², BELÉN TERCERO², AND EVELYNE ROUEFF³

Draft version April 24, 2022

ABSTRACT

We report on the first detection in space of fulminic acid, HCNO. This isomer of HNCO has been observed in three starless cores, B1, L1544 and L183, and in the low mass star forming region L1527 with a measured abundance ratio of HNCO/HCNO between 40-70. However, HCNO was not detected towards the direction of the cyanopolyne peak of TMC-1 or towards the Orion Hot Core region. The derived HNCO/HCNO abundance ratio in these cases is greater than 350 and 1000 in TMC-1 and Orion, respectively. We find that $\text{CH}_2 + \text{NO} \rightarrow \text{HCNO} + \text{H}$ is a key reaction for the formation of fulminic acid. A value of $5.5 \times 10^{-12} \text{ cm}^3 \text{ s}^{-1}$ of the corresponding reaction rate coefficient, as given by Miller et al. (2003), allows to reproduce the observed abundances of fulminic acid in both the observed dark clouds and low mass star forming core, where the determined abundance of HNCO in these regions with respect to molecular hydrogen is $1-5 \times 10^{-10}$.

Subject headings: astrochemistry — line: identification — ISM: abundances — ISM: clouds — ISM: molecules

1. INTRODUCTION

Isocyanic acid (HNCO) was first detected towards Sgr B2 (Snyder & Buhl 1972) and its rotational transitions have been found to be prominent towards the molecular clouds of the Galactic Center (Kuan & Snyder 1996; Cummins et al. 1986; Turner 1991; Martín et al. 2008). Since then, it has been observed towards dense cores associated with massive star formation (Jackson et al. 1984; Churchwell et al. 1986; Zinchenko et al. 2000), in the direction of TMC-1 (Brown 1981; Kaifu et al. 2004), in diffuse clouds (Turner et al. 1999) and in external galaxies (Meier & Turner 2005; Martín et al. 2006). Hence, isocyanic acid is found in a large variety of physical environments. In the 3 mm line survey we have performed in four dark cloud cores using the IRAM 30-m telescope (Marcelino et al. 2007a,b) we detected HNCO in all the observed sources, showing that this species is a common constituent of dark clouds. While its abundance in dark and diffuse clouds is $\simeq 10^{-10}$ (Turner 1991), in hot cores, the Galactic Center clouds and in external galaxies it is $\simeq 1 - 5 \times 10^{-9}$ (Zinchenko et al. 2000; Martín et al. 2006, 2008; Meier & Turner 2005).

HNCO has several isomers with a singlet electronic state: HOCN, HCNO, HONC, and HNOC. The chemical pathways leading to those isomers could be very different, since there is not an obvious common precursor. Thus, their detection in space could provide some information on the chemistry of these species. Unfortunately, only HNCO and HCNO have been fully characterized in the spectroscopic laboratories so far (see below). In this Letter we report on the first detection of fulminic acid,

¹ This work was based on observations carried out with the IRAM 30-meter telescope. IRAM is supported by INSU/CNRS (France), MPG (Germany) and IGN (Spain)

² DAMIR, Instituto de Estructura de la Materia, CSIC, Serrano 121, 28006 Madrid, Spain; nuria@damir.iem.csic.es, cerni@damir.iem.csic.es, belen@damir.iem.csic.es.

³ Observatoire de Paris-Meudon, LUTH UMR 8102, 5 Place Jules Janssen, F-92195 Meudon Cedex, France; evelyne.roueff@obspm.fr.

HCNO, towards B1, L1544, L183 and L1527.

2. OBSERVATIONS AND RESULTS

The observations were performed using the IRAM 30-m telescope (Granada, Spain) between 2002 December and 2007 February, and in 2008 July. We used two 3 mm SIS receivers working simultaneously at the same frequency, but with orthogonal polarizations. Both receivers were tuned in single sideband mode with image rejections ~ 24 dB. System temperatures were ~ 150 K, for the lowest frequencies and between 200–250 K for the highest ones. The observations were done in frequency switching mode. The spectrometer was an autocorrelator with 40 kHz of spectral resolution ($\sim 0.13 \text{ km s}^{-1}$). Intensity calibration was performed using two absorbers at different temperatures. The atmospheric opacity was obtained from the measurement of the sky emissivity and the use of the ATM code (Cernicharo 1985). Weather conditions were typically average summer conditions (water vapor column ~ 5 mm and zenith opacities ≤ 0.1 at 3 mm), except for the period in 2008 July when we had very good weather conditions (< 2 mm of precipitable water and opacities ~ 0.03).

Pointing and focus were checked, on strong and nearby sources, every 1.5 and 3 hours respectively. At the observed frequencies the beamwidth of the antenna is in the range $26'' - 22''$ and the main beam efficiency is $0.77 - 0.74$. The sources being similar in size, or slightly larger, than the main beam of the telescope, the contribution of the error beam to the observed intensities is negligible and all the spectra have been calibrated in main beam temperature scale. The observed lines are shown in Figure 1 and the derived line parameters, obtained from gaussian fits using the GILDAS package⁴, are resumed in Table 1.

During the 3 mm line survey (85.9–93.1 GHz) of the dark clouds B1, L1544, L183 and TMC-1, we have detected several unidentified lines. Among them one line at 91.751 GHz was observed toward all sources except

⁴ <http://www.iram.fr/IRAMFR/GILDAS>

TABLE 1
HCNO AND HCNO OBSERVED LINE PARAMETERS

Species	$\int T_{\text{MB}} dv$ (K km s ⁻¹)	V_{LSR} (km s ⁻¹)	Δv (km s ⁻¹)	T_{MB} (K)
Barnard 1				
HCNO				
(4-3)	0.065 (4)	6.635 (25)	1.003 (57)	0.061 (6)
(5-4)	0.064 (5)	6.604 (43)	1.053 (92)	0.057 (10)
HCNO				
(4 ₀₄ -3 ₀₃)	0.722 (6)	6.608 (4)	1.060 (10)	0.640 (5)
(5 ₀₅ -4 ₀₄)	0.728 (7)	6.628 (5)	0.934 (12)	0.732 (15)
L1527 (0,0)				
HCNO				
(4-3)	0.020 (2)	5.924 (20)	0.387 (40)	0.049 (6)
(5-4)	0.023 (2)	5.942 (31)	0.564 (60)	0.038 (7)
HCNO				
(4 ₀₄ -3 ₀₃)	0.180 (4)	5.942 (4)	0.386 (10)	0.439 (12)
(5 ₀₅ -4 ₀₄)	0.181 (7)	5.945 (5)	0.304 (13)	0.559 (24)
L1527 (20'', -20'')				
HCNO				
(4-3)	0.016 (3)	6.036 (33)	0.450 (92)	0.034 (7)
HCNO				
(4 ₀₄ -3 ₀₃)	0.068 (4)	5.955 (10)	0.310 (21)	0.208 (15)
(5 ₀₅ -4 ₀₄)	0.076 (7)	5.926 (14)	0.329 (34)	0.217 (24)
L1544				
HCNO				
(4-3)	0.018 (2)	7.073 (24)	0.420 (64)	0.040 (6)
HCNO				
(4 ₀₄ -3 ₀₃)	0.359 (2)	7.220 (1)	0.455 (3)	0.741 (6)
(5 ₀₅ -4 ₀₄)	0.247 (6)	7.180 (5)	0.419 (11)	0.554 (21)
L183				
HCNO				
(4-3)	0.016 (3)	2.554 (34)	0.356 (85)	0.041 (9)
HCNO				
(4 ₀₄ -3 ₀₃)	0.239 (2)	2.393 (2)	0.399 (4)	0.564 (6)
(5 ₀₅ -4 ₀₄)	0.183 (5)	2.414 (4)	0.307 (9)	0.561 (17)
TMC-1 (CP)				
HCNO				
(4 ₀₄ -3 ₀₃)	0.322 (3)	5.824 (4)	0.687 (8)	0.441 (8)
(5 ₀₅ -4 ₀₄)	0.217 (5)	5.889 (7)	0.531 (15)	0.384 (16)

NOTE. — Number in parentheses are 1σ uncertainties in units of the last digits. Adopted rest frequencies (MHz) for the observed lines are 91751.320 ± 0.004 & 114688.383 ± 0.005 for HCNO $J = 4-3$ and $5-4$ respectively, and 87925.240 ± 0.030 & 109905.757 ± 0.030 for HNC $4_{04} - 3_{03}$ and $5_{05} - 4_{04}$ respectively.

TMC-1. The observed frequency was not found in the available molecular catalogs: JPL (Pickett et al. 1998), CDMS (Müller et al. 2001, 2005), and NIST (Lovas 1992, 2004). Using a personal spectral line catalog developed by one of us (J. Cernicharo), we tentatively identified this line as the transition $J = 4-3$ of fulminic acid (HCNO). The frequencies of this species have been measured in the laboratory up to $J_{up} = 12$, corresponding to $\nu_{max} = 275.2$ GHz, by Winnewisser & Winnewisser (1971). The agreement between the frequency measured in the laboratory for the $J = 4-3$ transition and that observed in dark clouds was better than 30 kHz, i.e., similar to the uncertainty of the laboratory measurements and of the velocity determination in these objects. Within the survey frequency range we have also observed the $4_{04} - 3_{03}$ transition of HNC in all sources, including TMC-1. Frequencies for HNC have been computed from the effective rotational constants obtained recently by Lapinov et al. (2007).

In order to confirm the new detection we had additional observations with the IRAM 30-m radio telescope in 2008 July. We improved the S/N ratio on the $J = 4-3$ tran-

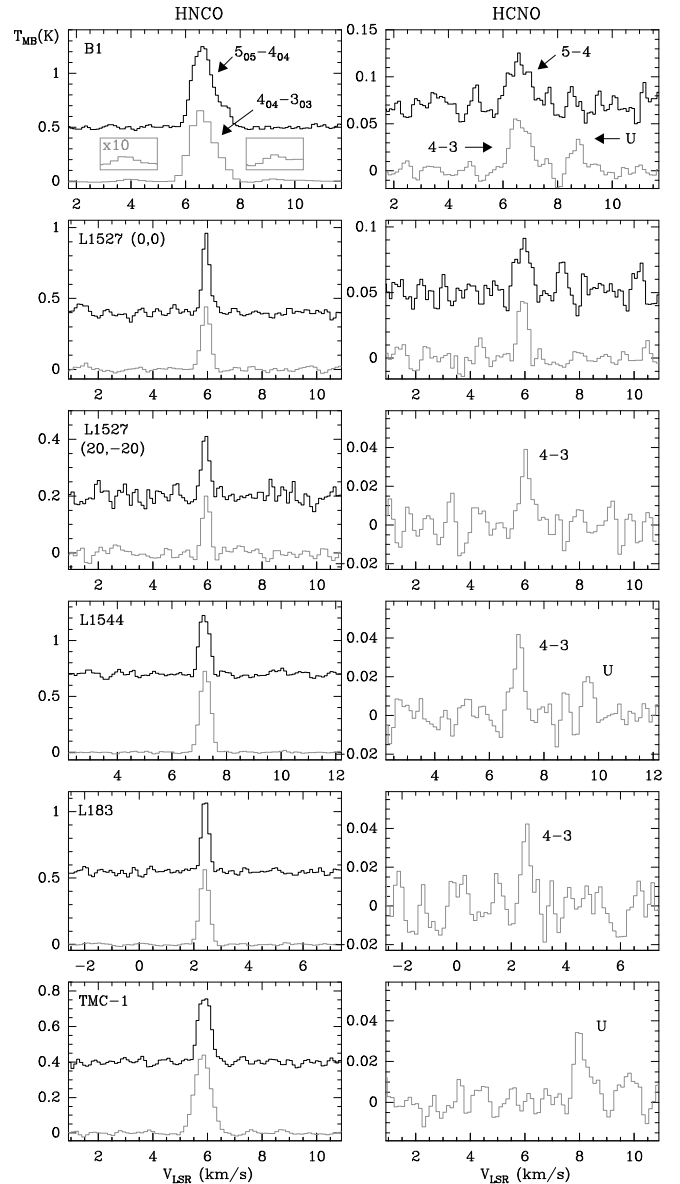


FIG. 1.— Line profiles for the observed transitions of HNC (left panel), and HCNO (right panel). Grey lines represent the HNC ($4_{04} - 3_{03}$) and HCNO ($4 - 3$) lines, while the black ones are for the HNC ($5_{05} - 4_{04}$) and HCNO ($5 - 4$) transitions. In B1, the hyperfine components of HNC ($4_{04} - 3_{03}$) at 4 and 9 km s⁻¹ are shown. Note the non detection of HCNO ($4 - 3$) towards TMC-1, and the presence of a unidentified line in this source, L1544 and B1 at 91750.68 ± 0.03 MHz.

sition, and observed the $J = 5-4$ towards the sources where the previous one was detected. We also included in this run L1527 to our targets. This source hosts a Class 0/I protostar and lately has been of great interest because of its strong lines of carbon-chain species (Sakai et al. 2007, 2008). In this source we have observed two positions, the central one towards the direction of the protostar, and another one located at an offset of $(20'', -20'')$, where the emission of carbon chains is still intense (see, Sakai et al. 2008). The observation of these two positions in L1527 could permit to distinguish between the emission in the region around the protostar and that of the cold envelope. We have also observed in this run another transition arising from HNC, in or-

TABLE 2
DERIVED COLUMN DENSITIES FOR HCNO AND HNCO.

Source	$N(\text{HCNO})$ 10^{10} cm^{-2}	$N(\text{HNCO})$ 10^{12} cm^{-2}	$n(\text{H}_2)$ 10^5 cm^{-3}	R
B1	21(1)/17(4)	9(1)/8(2)	6(1)	42/47
L1527	6(1)/4(1)	2.2(6)/1.8(4)	5(1)	37/40
L1527-B	5(1)/4(1)	0.9(5)/0.8(2)	5(1)	18/20
L1544	8(3)/6(2)	5(1)/4(1)	0.7(2)	62/66
L183	6(2)/5(1)	3.4(3)/2.5(6)	0.5(1)	57/50
TMC-1	$\leq 1.3/\leq 1.4$	5.7(4)/4(1)	0.3(1)	$> 390/320$
Orion-KL	≤ 890	9000(2000)		> 1000

NOTE. — R is the HNCO/HCNO abundance ratio. Errors to the column density are in parentheses in units of the last digit. L1527-B corresponds to the position (20'', -20'') of this source. The first entry in $N(\text{HCNO})$, $N(\text{HNCO})$, and R corresponds to the values obtained from the rotational diagrams, while the second one corresponds to those obtained from the *LVG* calculations.

der to derive volume densities, column densities, and the abundance ratio between both isomers.

Figure 1 shows the observed profiles for the HNCO and HCNO transitions. The $J = 4 - 3$ transition of HCNO is clearly detected in B1, L1544, L183 and L1527 well above 6σ level. However, it was not detected towards the direction of the cyanopolyne peak of TMC-1, with an rms of 6 mK. The $J = 5 - 4$ transition was detected only towards B1 and L1527 with similar intensities than those of the $4 - 3$ line. Upper limits (3σ) to the $J = 5 - 4$ line intensity are < 0.010 K, < 0.012 K, and < 0.018 K for L1527 (20'', -20''), L1544, and L183 respectively. This line should be 2-2.5 times weaker than the $J = 4 - 3$ transition, which is consistent with the intensity ratios for HNCO in these sources.

3. DISCUSSION

The dipole moment of fulminic acid is 3.099 D (Takashi et al., 1989), while that of HNCO is 2.1 ($\mu_a=1.60$ D, $\mu_b=1.35$ D; Hocking et al. 1974). Consequently, both molecules could have different excitation conditions and we have performed rotational diagrams in order to obtain rotational temperatures (T_{rot}) and column densities (N). Two transitions of HNCO were observed in all the sources. The fit of both lines gives rotational temperatures of 12 ± 3 K, 12 ± 4 K, 15 ± 6 K, 6 ± 1 K, 7 ± 1 K and 6 ± 1 K for B1, L1527 (0, 0), L1527 (20'', -20''), L1544, L183 and TMC-1, respectively. Errors to the derived temperatures and column densities include those obtained from the gaussian fit, calibration errors and the fact that we are using only two transitions to perform the rotational diagram. Although HNCO presents hyperfine structure, we have not included it in our calculations since it is only important for low rotational quantum numbers ($J < 3$). Nevertheless, two weak hyperfine lines are visible towards B1 in the $4_{04}-3_{03}$ transition at 4 and 9 km s $^{-1}$ (see Fig. 1). They are ten times weaker than the strongest component indicating that the HNCO lines are optically thin. B1 and the central position of L1527 are the only sources where two transitions of fulminic acid have been detected, and where we have estimated rotational temperatures of 10 ± 4 K and 17 ± 8 K respectively. For the other three sources T_{rot} has been assumed to be the same for both isomers. Table 2 shows the obtained column den-

sities for HCNO and HNCO, and the abundance ratio between both isomers.

Collisional rates for HNCO are available from Green's calculations⁵. We have used a Large Velocity Gradient code to derive volume and column densities for HNCO and HCNO in order to better constraint the HNCO/HCNO abundance ratio (hereafter referred to as R). The collisional rates $J \rightarrow J'$ for HCNO are unknown but we have assumed that they are identical to the $J_{0J} \rightarrow J'_{0J'}$ collisional rates of HNCO. The adopted kinetic temperatures are 10 K for all dark clouds except B1 and L1527 for which we have assumed $T_{\text{kin}} = 15$ K following the rotational temperatures derived above from HNCO. The obtained values for $n(\text{H}_2)$, $N(\text{HNCO})$ and $N(\text{HCNO})$ are also given in Table 2. Errors to the *LVG* calculations are estimated to be about 25 %. The agreement between the column densities derived from the two methods is very good.

In Orion-KL we have detected more than 60 spectral lines of HNCO at 3, 2 and 1.3 mm (see the line survey of Orion by Tercero et al., 2008, in preparation). Column densities have been calculated using LTE approximation included in radiative transfer codes developed by J. Cernicharo (Cernicharo 2008, in preparation). We have kept constant the physical properties of each component of Orion-KL (extended ridge, compact ridge, plateau and hot core; see Blake et al. 1987 for the standard values we have assumed) including their sizes and offsets with respect IRC2 (survey pointing position). Corrections for beam dilution are applied for each line. We have estimated the uncertainty to be about 25 %, considering error sources as the line opacity effects, the simplification of the model, the division of the whole line emission in different components and pointing and calibration errors. The results are $(1.5 \pm 0.4) \times 10^{14}$, $(1.5 \pm 0.4) \times 10^{15}$, $(1.0 \pm 0.3) \times 10^{15}$ and $(7 \pm 2) \times 10^{14} \text{ cm}^{-2}$ for the extended ridge, the plateau, the compact ridge and the hot core respectively. For the hot core a second component with $T_{\text{kin}}=300 \pm 75$ K and $N(\text{HNCO})=(6 \pm 2) \times 10^{15} \text{ cm}^{-2}$ is needed to reproduce the observations. In none of these components HCNO has been detected. The upper limit to R is 1100 in the hot core, the plateau and the compact ridge, and 300 in the extended ridge. Since the Orion region is dominated by grain-surface chemistry –which explains the large column density of HNCO– rather than ion-molecule and neutral-neutral gas phase reactions, the lack of HCNO suggests that grain surface chemistry is not the main path to the production of HCNO in molecular clouds (see below).

From recent state of the art *ab initio* calculations, the relative energies of HOCN, HCNO and HONC, in their ground electronic singlet states, compared to HNCO, are 24.7, 70.7 and 84.1 kcal mol $^{-1}$ at an unprecedented level of accuracy (Schuurman et al. 2004). Another isomer, HNOC, is predicted by *ab initio* calculations at ≈ 135 kcal mol $^{-1}$ above HNCO (Mebel et al. 1996). The relative abundance of the different isomers in molecular clouds depend on the chemical paths leading to their formation. Unlike the case of HCN/HNC, which are mainly formed from the dissociative recombination of HCNH^+ , there is not an obvious common parent molecule leading to the simultaneous formation of the various HNCO iso-

⁵ unpublished results, see <http://molscat.giss.nasa.gov>

TABLE 3
MODEL ABUNDANCES OBTAINED FOR THE HNCO ISOMERS IN
COLD CLOUDS

$n(\text{H}_2)$ 10^4 cm^{-3}	NO 10^{-7}	HNCO 10^{-10}	HCNO 10^{-11}	HOCN 10^{-13}	NCO 10^{-8}	R
0.1	0.005	0.004	0.04	0.47	0.02	0.8
0.3	0.01	0.01	0.08	1.30	0.07	1.5
1.0	8.6	18	6.30	38.0	6.6	29
3.0	7.4	18	3.10	12.0	4.5	58
10	5.1	9.3	1.20	2.0	2.0	72
30	3.2	3.4	0.58	0.31	0.8	58
50	2.5	2.0	0.41	0.13	0.5	49
100	1.7	0.9	0.25	0.04	0.3	36

NOTE. — R is the HNCO/HCNO abundance ratio

mers. The most evident formation path for HNCO and HCNO could be the reaction of HCNH^+ with atomic oxygen and OH. Unfortunately, it has been shown in the laboratory that HCNH^+ does not react with oxygen (Scott et al. 1999) and nothing is known about its reaction with OH. Iglesias (1977) suggested the reaction $\text{NCO}^+ + \text{H}_2 \rightarrow \text{HNCO}^+ + \text{H}$ as a starting point for the chemistry of HNCO. The other isomers can not be produced via this reaction as the corresponding channels are endothermic. We have introduced a tentative gas phase chemical network with the three most stable isomers – HNCO, HOCN and HCNO – and their associated ions which have been studied theoretically by Luna et al. (1996). We have obtained that the proton transfer reactions involving H_3^+ and NCO, the most stable isomer, could lead to both HCNO^+ and HOCN^+ via exothermic channels. The HNCO^+ , HCNO^+ and HOCN^+ ions can further react with molecular hydrogen, giving respectively H_2NCO^+ , H_2CNO^+ and HOCNH^+ , whose relative energies have been computed by Hop et al. (1989). These ion-molecule reactions are followed by dissociative recombination where we assume that no chemical structural change occurs so that $\text{H}_2\text{NCO}^+/\text{H}_2\text{CNO}^+ + e^- \rightarrow \text{HNCO}/\text{HCNO} + \text{H}$, and $\text{HOCNH}^+ + e^- \rightarrow \text{HNCO}/\text{HOCN} + \text{H}$.

Neutral-neutral reactions may also be at work. So, HNCO can be formed by $\text{CN} + \text{O}_2 \rightarrow \text{NCO} + \text{O}$, followed by $\text{NCO} + \text{H}_2 \rightarrow \text{HNCO} + \text{H}$, as suggested by Turner (2000). However the presence of an activation barrier in the $\text{NCO} + \text{H}_2$ reaction can not be dismissed and a tentative barrier of 500 K is introduced in the present work. In addition, a favorable neutral-neutral pathway leading to the formation of HCNO is provided by $\text{CH}_2 + \text{NO} \rightarrow \text{HCNO} + \text{H}$, a reaction well studied in combustion and atmospheric chemistry (Glarborg et al. 1998), for which no activation barrier has been found by Roggenbuck & Temps (1998) from *ab initio* studies. Other neutral-neutral reactions of HCNO in the presence of atomic oxygen and NO may occur (Miller et al. 2003). Including these various possibilities in a chemical network, we have computed equilibrium solutions

by solving directly the steady state chemical equations. Table 3 displays the fractional abundances relative to molecular hydrogen for different volume densities in cold clouds, at a temperature of 10 K and a cosmic ionization rate of $5 \times 10^{-17} \text{ s}^{-1}$. These results do not differ considerably when assuming a temperature of 15 K and 20 K. The predicted abundance for NO is in good agreement with the value observed in dark clouds (Gerin et al. 1992, 1993). NCO has also a large abundance, but due to its moderate dipole moment (0.67 D) and a $^2\Pi$ structure diluting the emission spectrum resulting from an enhanced partition function, the expected intensity from its rotational lines is rather weak. From our line survey of dark clouds (Marcelino et al. 2007a,b) we derive limits to its abundance of $1\text{-}5 \times 10^{-9}$. The result from our models show a good agreement with the values observed for R in dark clouds and low-mass star forming regions. It increases with volume density up to $n(\text{H}_2) = 10^5 \text{ cm}^{-3}$, but decreases again when the density is larger than this value. It seems that for low and high volume density clouds fulminic acid could be rather abundant, while in clouds of moderate density, like TMC-1, it will be much less abundant than isocyanic acid, HNCO. Furthermore TMC-1 shows a very peculiar chemistry, being a carbon rich source while it is deficient in oxygen bearing species. That could be the reason why HCNO is detected in L183, similar to TMC-1 in density and temperature but oxygen rich, and not towards TMC-1. The formation of HNCO on dust grains may also be very efficient (Hasewaga & Herbst 1993) and these surface chemistry processes could also lead to the formation of HCNO (Herbst, private communication). However, the gas phase models predict abundances for HNCO very close to those observed in dark clouds. Moreover, these models also predict the observed HNCO/HCNO abundance ratio. The detection of the different isomers of HNCO provides a fundamental information concerning the physical and chemical conditions, in particular the respective contribution of gas phase and grain processes in the chemistry since there is not an obvious common precursor for them. Thus, the observation of the other isomer of HNCO, HOCN, for which present gas phase models predict a very low abundance in dark clouds could provide a good discrimination between gas and grain surface processes in dark clouds. The search for HNCO isomers towards different environments would be the next step to further investigate their chemical production.

We would like to thank Eric Herbst for useful comments and suggestions, and Marcelino Agúndez for carefully reading of the paper. We also thank our anonymous referee, whose detailed comments have helped to improve the paper. This work has been supported by Spanish Ministerio de Ciencia e Innovación through grants AYA2003-2785, AYA2006-14876, and by DGU of the Madrid community government under IV-PRICIT project S-0505/ESP-0237 (ASTROCAM).

REFERENCES

- Blake, G.A., Sutton, E.C., Masson, C.R., & Philips, T.H. 1987, *ApJ*, 315, 621
 Brown, R.L. 1981, *ApJ*, 248, 119
 Cernicharo, J. 1985, IRAM report No. 52 (Granada:IRAM)
 Churchwell, E., Wood, D., Myers, P.C., & Myers, R.V. 1986, *ApJ*, 305, 405
 Cummins, S.E., Linke, R.A., & Thaddeus, P. 1986, *ApJS*, 60, 819

- Gerin, M., Viala, Y., Pauzat, F., & Ellinger, Y. 1992, *A&A*, 266, 463
- Gerin, M., Viala, Y., & Casoli, F. 1993, *A&A*, 268, 212
- Glarborg, P., Alzueta M.U., Dam-Johansen K., & Miller J.A. 1998, *Combustion and Flame*, 115, 1
- Hasewaga, T.I., & Herbst, E., 1993, *MNRAS*, 263, 589
- Hocking, W.H., Gerry M.C.L., & Winnewisser, G. 1974, *ApJ*, 187, L89
- Hop C.E.C.A., Holmes J.L., Rutting P.J.A., Schaftenaar G., & Terlouw J.K. 1989, *Chem. Phys. Lett.*, 156, 251
- Iglesias, E., 1977, *ApJ*, 218, 697
- Jackson, J.M., Armstrong, J.T., & Barrett, A.H. 1984, *ApJ*, 280, 608
- Kaifu, N., Ohishi, M., Kawaguchi, K., et al. 2004, *PASJ*, 56, 69
- Kuan, Y.-J., & Snyder, L.E. 1996, *ApJ*, 470, 981
- Lapinov, A.V., Golubiatnikov, G.Y., Markov, V.N., & Guarnieri, A., 2007, *Astron. Letters*, 33, 121
- Lovas, F.J. 1992, *J. Phys. Chem. Ref. Data*, 21, 181
- Lovas, F.J. 2004, *J. Phys. Chem. Ref. Data*, 33, 177
- Luna A., Mebel A.M., & Morokuma K. 1996, *J. Chem. Phys.*, 105, 3187
- Marcelino, N., Cernicharo, J., Agúndez, M., et al. 2007a, *ApJ*, 665, 127
- Marcelino, N., 2007b, PhD Thesis, “Estudio de la Química en Nubes Oscuras”, University of Granada.
- Martín, S., Mauersberger, R., Martín-Pintado, J., Henkel, C. & García-Burillo, S. 2006, *ApJS*, 164, 450
- Martín, S., Requena-Torres, M.A., Martín-Pintado, J., & Mauersberger, R. 2008, *ApJ*, 678, 245
- Mebel, A.M., Luna, A., Lin, M.C., & Morokuma, K., 1996, *J. Chem. Phys.*, 105, 6439
- Meier, D.S., & Turner, J.L. 2005, *ApJ*, 618, 259
- Miller J.A., Klippenstein S.J., & Glarborg P. 2003, *Combustion and Flame*, 135, 357
- Müller, H.S.P., Thorwirth, S., Roth, D.A., & Winnewisser, G. 2001, *A&A*, 370, L49
- Müller, H.S.P., Schlöder, F., Stutzki, J., & Winnewisser, G. 2005, *J. Mol. Struct.*, 742, 215
- Pickett, H.M., Poynter, R.L., Cohen, E.A., et al. 1998, *J. Quant. Spec. Radiat. Transf.*, 60, 883
- Roggenbuck, J., & Temps, F., 1998, *Chem. Phys. Lett.*, 285, 422
- Sakai, N., Sakai, T., Osamura, Y., & Yamamoto, S. 2007, *ApJ*, 667, 65
- Sakai, N., Sakai, T., Hirota, T., & Yamamoto, S. 2008, *ApJ*, 672, 371
- Schuurman, M.S., Muir, S.R., Allen, W.D., & Schaefer III, H.F., 2004, *J. Chem. Phys.*, 120, 11587
- Scott, G.B.I., Fairley, D.A., Milligan, D.B., Freeman, C.G., & McEwan, M.J., 1999, *J. Phys. Chem. A*, 1999, 103, 7470
- Snyder, L.E., & Buhl, D. 1972, *ApJ*, 177, 619
- Takashi, R., Tanaka, K., & Tanaka, T., 1989, *J. Mol. Spectrosc.*, 138, 450
- Turner, B.E. 1991, *ApJS*, 76, 617
- Turner, B.E., Terzieva, R., & Herbst, E. 1999, *ApJ*, 518, 699
- Turner, B.E. 2000, *ApJ*, 542, 837
- Zinchenko, I., Henkel, C., & Mao, R. Q. 2000, *A&A*, 361, 1079
- Winnewisser, M. & Winnewisser, B.P., 1971, *Z. Naturforsch*, 26a, 128